Density functional theory and atoms-in-molecule study on the role of two-electron stabilizing interactions in retro Diels–Alder reaction of cycloadducts derived from substituted cyclopentadiene and *p*-benzoquinone†

Mahendra P. Patil and Raghavan B. Sunoj*

Received 31st July 2006, Accepted 6th September 2006
First published as an Advance Article on the web 27th September 2006
DOI: 10.1039/b610972a

A systematic investigation on the cycloreversion reaction of the cycloadduct formed between substituted cyclopentadiene and *p*-benzoquinone (**1**–**19**) is reported at the B3LYP/6-311+G**//B3LYP/6-31G* level of theory. The computed activation barrier exhibits a fairly high sensitivity to the nature of substituents at the C_7-position. Gibbs free energy of activation for **1** and **19** are found to be 20.3 and 30.1 kcal mol^{-1}, respectively, compared to **7**, which is estimated to be 24.7 kcal mol^{-1}. Quantitative analysis of the electronic effects operating in both the cycloadduct as well as the corresponding transition state for the retro Diels–Alder (rDA) reaction performed using the natural bond orbital (NBO) and atoms in molecule (AIM) methods have identified important two-electron stabilizing interactions. Among four major delocalizations, $\sigma(C_7–X)$ to $\sigma^*(C_1–C_5)$ [and to $\sigma^*(C_2–C_6)$] is identified as the key contributing factor responsible for ground state $C_1–C_5$ bond elongation, which in turn is found to be crucial in promoting the rDA reaction. A good correlation between the population of antibonding orbital [$\sigma^*(C_1–C_5)$] of the ground state cycloadduct and Gibbs free energy of activation is observed. The importance of factors that modulate ground state structural features in controlling the energetics of rDA reaction is described.

Introduction

The retro Diels–Alder reaction (rDA) is an important class of pericyclic reaction, which gained considerable attention over the years both from experimental as well as theoretical groups. The earliest reports on the reverse of the Diels–Alder reaction date back to its very discovery, where the cycloadduct formed between furan and maleic anhydride was found to undergo dissociation near its melting point.[1] While rDA reactions are often reported as an issue under elevated temperatures, a more programmed approach was able to exploit the potential of this reaction. Numerous examples have been reported on the practical utility of rDA reactions as a ring opening strategy in the total synthesis of many natural products as well as heterocyclic compounds.[2] The Diels–Alder/retro Diels–Alder reaction sequence is frequently employed in masking double bonds on the dienophile and subsequent regeneration after successfully carrying out other functional group transformations elsewhere in the dienophile.[3] The rDA normally require the use of high temperatures or flash vacuum thermolysis (FVT) techniques, which are not suitable for many dienes and monomers owing to decomposition issues of reactants prior to the desired rDA reaction.[4] There have been interesting reports in the recent literature on low temperature rDA reactions with functionalized fulvenes as the diene component.[5] Reversible Diels–Alder reactions have also been exploited in order to synthesize certain biologically active compounds[5] and dendrimers,[6] where rDA reactions are carried out at relatively lower temperatures by careful choice of the diene. It is of inherent interest to unravel the factors that could directly influence the energetics of the rDA reaction so as to achieve milder reaction conditions and faster rates.

A large number of studies aimed at establishing the mechanism of these reactions,[7] the role of substituents in determining stereoselectivity[8] and π-facial selectivity[9] has been found in the literature. Questions related to the concerted *versus* step-wise mechanism for Diels–Alder reactions remained as a topic for several leading discussions.[10] Through their theoretical studies, Houk *et al.* suggested that concerted mechanisms are, in general, favored by about 3–7 kcal mol^{-1} over the step-wise pathway.[11] Zewail and co-workers have studied rDA reactions using a femtosecond dynamics method, which suggested that both trajectories (concerted and step-wise) are possible in these reactions, but acceptance of the favorable mechanism needs careful geometrical analysis of the reactants, the location of the transition state and the barrier height of reaction.[12]

Structure and energetics of molecules in the ground state as well as the transition state can provide valuable information on chemical reactions. As part of our continued effort in exploring the substituent effects in rDA reactions, we have decided to investigate a simple cycloadduct that could serve as synthetic equivalent for masked double bonds. Magnus *et al.* assigned the 'β-silyl effect' as the primary reason behind the observed rate

Department of Chemistry, Indian Institute of Technology Bombay, Powai, Mumbai, 400076, India. E-mail: sunoj@chem.iitb.ac.in; Fax: +91 (0)22 2576 7152

† Electronic supplementary information (ESI) available: The B3LYP/6–31G* optimized geometries for all the stationary points in the form of Cartesian coordinates, total electronic energies, zero-point corrected energies, vibrational frequencies, details on NBO, AIM calculations and correlation between Marcus intrinsic barriers with structural parameters. See DOI: 10.1039/b610972a

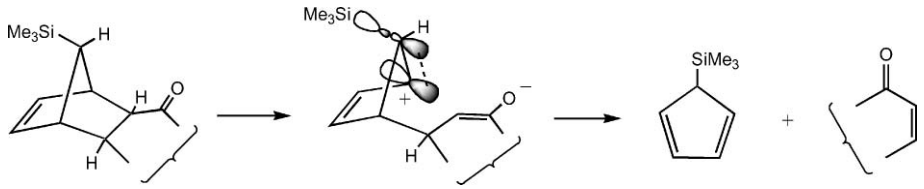

Scheme 1

enhancement in the rDA reaction for trimethylsilyl substituted cycloadducts by considering a polarized transition state in a step-wise mechanism (Scheme 1).[13]

Another interesting report closely pertaining to the present thesis is due to White and co-workers, where they have demonstrated that ground state geometries could have a profound effect on the observed rate enhancement in the rDA reaction for a range of cyclopentadiene and cyclohexadiene cycloadducts.[14] Cycloadducts **a** and **c**, that undergo a facile rDA reaction upon heating, were found to have elongated C_1–C_2 bonds at the ground state compared to their saturated analogues **b** and **d** (Chart 1).

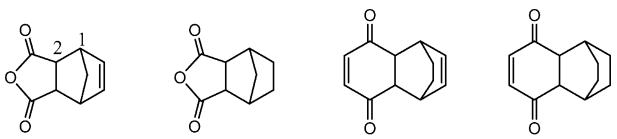

a **b** **c** **d**

Chart 1

In a very recent study, Kotha *et al.* have demonstrated how an orbital interaction protocol can effectively be employed in reducing the kinetic barrier associated with the cyclo-reversion process which can help achieve the rDA reaction under milder experimental conditions.[15] Consideration of the increasingly popular applications of the rDA reaction and the lack of systematic investigations on the energetics of this reaction as a function of the substituents, prompted us to investigate the importance of structural features in the ground state and the corresponding relationship with the reaction energetics. Herein, we report a systematic study on the effect of substituents on the rDA reaction of cycloadducts formed between substituted cyclopentadiene and *p*-benzoquinone based on the hybrid Hartree–Fock density functional theory method.

Computational methods

Potential energy surfaces have been explored using the B3LYP/6-31G* level of theory using the GAUSSIAN 98 suite of quantum chemical programs.[16] Performance of hybrid-HF DFT methods (such as B3LYP), particularly for pericyclic reactions, has been quite impressive.[17] All geometries were fully optimized and have been characterized as stationary points on the potential energy surface at the same level of theory by evaluating corresponding Hessian indices. Single point energies have been computed with a more flexible basis set, namely, the 6-311+G**. All the energies are reported at the B3LYP/6-311+G**//B3LYP/6-31G* level of theory. Zero-point vibrational energies (at the B3LYP/6-31G* level) have been scaled by 0.9806 and are included in the reported energies.[18] Transition states of cycloreversion reactions have been characterized by the unique imaginary frequency pertaining to the reaction coordinate. Further, we have carried out 10% geometric displacement of the transition state geometry along the direction of the imaginary vibrational frequency and subsequently reoptimized using 'calcfc' option. This is to ensure whether the obtained transition state genuinely connects reactants and product. Intrinsic reaction coordinate (IRC) calculations have also been carried out to authenticate the transition state.[19] Weinhold's natural bond orbital analysis has been performed using the NBO5.0 program so as to probe the electron delocalization in detail.[20] Topological analysis with Bader's atoms in molecule analysis[21] (AIM) was carried out using AIM2000 software.[22] Both NBO and AIM analyses were performed on the wave function obtained at the B3LYP/6-311+G**//B3LYP/6-31G* level.

Results and discussion

We have chosen an interesting class of cycloadducts formed between cyclopentadiene and *p*-benzoquinone, with different substituents on the cyclopentadienyl unit (Scheme 2). These cycloadducts are ideal substrates in establishing the role of substituents on the kinetics of the rDA reaction. The energy barrier for the rDA for a variety of C_7 substituted systems has been calculated at the B3LYP/6-311+G**//B3LYP/6-31G* level of theory and the results are summarized in the following sections.

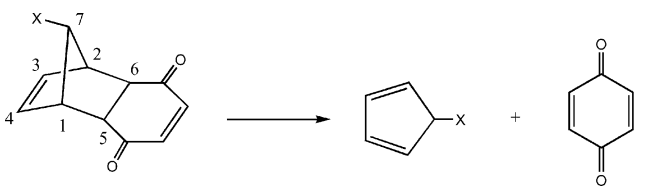

Scheme 2 Retro Diels–Alder reaction of the methano bridge-substituted (C_7) cycloadduct between substituted cyclopentadiene and *p*-benzoquinone.

Magnus *et al.* have elegantly demonstrated through their kinetic measurements that rDA reaction of the cycloadduct between 5-(trimethylsilyl)cyclopentadiene and *p*-benzoquinone, proceeds 95 times faster than the corresponding unsubstituted system (X = H) under comparable reaction conditions.[13] This evidently indicates that the barrier to rDA reaction for 7-trimethylsilyl substituted substrate should be fairly low, an observation reminiscent of the 'β-silyl effect' proposed to explain the stability of carbocations.[23] We believe that rDA reactions considered in the present study (**1** through **19**) will most likely proceed *via* a concerted pathway through a nearly symmetric transition state. Thus, the possibility for larger charge separation and concomitant stabilization of charge separated intermediates by β-silyl group can safely be excluded. While the rate acceleration offered by the –$SiMe_3$ group at the C_7 position is known, generalizations on how

Table 1 Key structural parameters obtained at the B3LYP/6-31G* level for the cycloadducts formed between substituted cyclopentadiene and *p*-benzoquinone[a]

Substituents	C_1–C_5	C_7–X	C_1–C_4	C_3–C_4	C_5–C_6
–$SiMe_3$(**1**)	1.587	1.915	1.521	1.341	1.558
–GeH_3 (**2**)	1.586	1.957	1.521	1.340	1.560
–BH_2 (**3**)	1.582	1.572	1.524	1.344	1.560
–PH_2 (**4**)	1.584	1.882	1.521	1.340	1.561
–CMe_3 (**5**)	1.584	1.555	1.520	1.340	1.562
–CHO (**6**)	1.581	1.513	1.522	1.340	1.560
–H (**7**)	1.583	1.094	1.522	1.341	1.560
–C_2H_5 (**8**)	1.581	1.531	1.521	1.340	1.560
–Me (**9**)	1.581	1.526	1.521	1.340	1.561
–SH (**10**)	1.581	1.833	1.521	1.341	1.563
–COMe (**11**)	1.579	1.528	1.523	1.341	1.562
–COOH (**12**)	1.579	1.515	1.523	1.341	1.562
–Cl (**13**)	1.581	1.810	1.521	1.339	1.564
–NH_2 (**14**)	1.577	1.450	1.523	1.342	1.563
–CN (**15**)	1.577	1.463	1.523	1.340	1.562
–OMe (**16**)	1.578	1.402	1.519	1.339	1.563
–NO_2 (**17**)	1.577	1.510	1.524	1.340	1.564
–OH (**18**)	1.575	1.403	1.521	1.344	1.563
–F (**19**)	1.577	1.380	1.521	1.340	1.565

[a] Atoms numbers are same as in Scheme 1.

different substituents could influence the rate of rDA reactions as well as the electronic origins behind observed rate enhancements are conspicuously absent. We have decided to probe in greater detail the fundamental reasons behind the rate acceleration by trimethylsilyl and a number of other substituents. An orbital interaction protocol is adopted to gain insight on the electronic effects operating both at the ground as well as the transition states.

First, investigation of the structural parameters of the cycloadducts is taken up with the immediate objective of identifying the role of substituents on the cycloadduct geometry. Optimized structural parameters containing key bond distances of the cycloadducts are summarized in Table 1.[24] In general, it can be noticed that the C_1–C_5 (and C_2–C_6) bond is much longer than a normal C–C single bond (*cf.* 1.537 Å for cyclohexane computed at the same level of theory). While the bond elongation can in part be attributed to the inherent strain in the bicyclo system, variation of bond length with respect the nature of substituents at the C_7 position appears interesting and warrants a detailed investigation. Another interesting observation relates to the C_1–C_5 elongation compared to the corresponding bond distance in a similar bicyclic compound with a saturated C_3–C_4 bond. For instance, substituents such as –$SiMe_3$ (**1**), increase the C_1–C_5 (and C_2–C_6) bond distance compared to the unsubstituted system (X = H) whereas, cyano (**15**) and fluoro (**19**) groups decrease the bond distance.[25] Such variations could have subtle consequences on the energetics of cycloreversion reactions, where C_1–C_5 and C_2–C_6 bonds are being cleaved. Other bond distances such as C_1–C_4 and C_3–C_4 show little sensitivity to the C_7 substituents. Interestingly, the C_1–C_5 bond distances in a saturated version (hydrogenated C_3–C_4 bond) of the same bicyclic compound show a uniformly shorter bond length (averaging around 1.56 Å) irrespective of the nature of C_7-substituents.[25] Probing the governing electronic factors behind substituent-dependent bond length variation in these substrates is intuitively appealing at this juncture. The natural bond orbital (NBO) analysis has been widely accepted as a useful tool to understand electronic interactions in molecules.[26] We have carried out an exhaustive search for key orbital interactions responsible for the structural features in these cycloadducts based on the NBO method and results are succinctly represented below.

The structural features in these cycloadducts offer antiperiplanar disposition of C_7–X and C_1–C_5 (and C_2–C_6) bonds that will help to maximize $\sigma_{(C-X)} \rightarrow \sigma^*_{(C-C)}$ filled–unfilled electronic interactions.[27] In case of the –$SiMe_3$ substituent, the second order perturbation stabilization energy arising due to two-electron stabilizing interaction is computed to be 1.72 kcal mol^{-1}. The ability of the antiperiplanar substituent –$SiMe_3$ to increase the population of the σ* antibonding orbital of C_1–C_5 (and C_2–C_6) bond is one of the key factors responsible for bond elongation. Contour diagram, **1**·**1**, generated using the NBO basis as given in Fig. 1, clearly depicts an effective 'filled–unfilled' orbital interaction between donor [σ(C_7–Si) bond] and acceptor orbitals [σ*(C_1–C_5)]. It is also noticed that the energy difference (ΔE) between interacting donor–acceptor orbitals in the trimethylsilyl system is smaller than with any other substituent, hence the interaction is expected to be better (Table 2). Examination of other electron delocalizations revealed that C_1–C_5 bond elongation is further assisted by π(C_3–C_4) to σ*(C_1–C_5) [and C_2–C_6] donation (**1**·**2**). The role of π(C_3–C_4) to σ*(C_1–C_5) donation has been verified by examining the structural parameters for the corresponding saturated bicyclic system (hydrogenated C_3–C_4 bonds) at the same level of theory. For example, when X = H, the C_1–C_5 bond distances are 1.561 and 1.583 Å, respectively, for saturated and unsaturated systems.[24] The extent of π(C_3–C_4) to σ*(C_1–C_5) and σ(C_1–C_5) to π*(C_3–C_4) donations has been found to remain nearly the same, irrespective of the nature of the X-group present at the C_7 position.[28] Another contributing factor depleting the σ(C_1–C_5) population is delocalization from C_1–C_5 to π*(C_3–C_4) (**1**·**3**) as well as to σ*(C_7–X) (**1**·**4**). All these four delocalizations are succinctly represented in Fig. 1 using contour diagrams generated with NBO basis. The net effect of all four delocalizations, first two involving σ*(C_1–C_5) as the acceptor orbital and another two interactions where σ(C_1–C_5) acts as donor orbitals, results in bond elongation compared to both saturated and unsubstituted (when X = H) analogues of this bicyclic system. The difference in population of σ*(C_1–C_5) bond across a number of systems considered here is found to be more sensitive to the nature of substituents attached to the C_7 position. For sake of brevity, we have included second order perturbation energies for only these delocalizations in Table 2. A complete set of orbital delocalizations is included in Table S2 in the ESI.†

Variations in bond elongation in the ground state cycloadducts are further probed by topological analysis of the electron density using the atoms in molecules (AIM) method.[20] Calculated properties of (3, −1) bond critical points along C_1–C_5 bond, such as electron density [$\rho(r_c)$], Laplacian of electron density [$\nabla^2\rho(r_c)$] and total energy density (H) are included in Table 2. Since the $\rho(r_c)$ values correspond to the strength of interaction, a lower value implies a weaker bonding. In the previous section we have highlighted the importance of C_3–C_4 unsaturation (along with other key delocalizations), contributing to the C_1–C_5 bond elongation. Thus, comparison of $\rho(r_c)$ values for the C_1–C_5 bonds with the corresponding values for the saturated analogues are carried out.[29] The $\rho(r_c)$ values are consistently found to be lower for the cycloadduct (**1** through **19**) compared to the saturated bicyclic compound (Table S3 in the ESI†), underscoring the presence of a weaker C_1–C_5 (and

Table 2 Summary of natural bond orbital (NBO) and atoms in molecule (AIM) analyses performed with wave functions generated at the B3LYP/6-311+G**//B3LYP/6-31G* level of theory

	NBO[a]			AIM[b]		
	$E^{(2)}$/kcal mol^{-1}					
Substituents	σ(C7–X) → σ*(C1–C5)	ΔE/au	σ*(C_1–C_5) occupancy	$\rho(r_c)$/ea$_0^{-3}$	$\nabla^2(r_c)$/ea$_0^{-5}$	H/ea$_0^{-4}$
–$SiMe_3$ (**1**)	1.72	0.80	0.03582	0.2144	0.1008	−3.135
–GeH_3 (**2**)	1.83	0.83	0.03547	0.2152	0.1018	−3.141
–BH_2 (**3**)	1.62	0.88	0.03368	0.2170	0.1041	−2.734
–PH_2 (**4**)	1.72	0.84	0.03348	0.2160	0.1028	−2.879
–CMe_3 (**5**)	0.74	0.91	0.03080	0.2159	0.1027	−3.087
–CHO (**6**)	1.03	0.96	0.03126	0.2175	0.1045	−2.862
–H (**7**)	1.81	0.82	0.03270	0.2164	0.1034	−2.631
–C_2H_5 (**8**)	1.00	0.93	0.03011	0.2171	0.1042	−2.875
–Me (**9**)	1.03	0.94	0.03032	0.2172	0.1044	−2.776
–SH (**10**)	1.23	0.92	0.03181	0.2172	0.1042	−2.901
–COMe (**11**)	1.05	0.96	0.02914	0.2186	0.1058	−2.992
–COOH (**12**)	1.13	0.98	0.02940	0.2190	0.1064	−3.006
–Cl (**13**)	1.10	0.98	0.03105	0.2172	0.1043	−2.909
–NH_2 (**14**)	0.87	1.07	0.02800	0.2189	0.1065	−2.805
–CN (**15**)	0.96	1.02	0.02974	0.2199	0.1075	−2.865
–OMe (**16**)	0.75	1.17	0.02763	0.2189	0.1068	−2.918
–NO_2 (**17**)	0.76	1.09	0.02957	0.2195	0.1071	−3.027
–OH (**18**)	0.61	1.18	0.02878	0.2194	0.1069	−2.818
–F (**19**)	0.62	1.29	0.02871	0.2189	0.1063	−2.817

[a] $E^{(2)}$ and ΔE are, respectively, second order perturbation energy and the energy gap between the donor and acceptor orbitals. [b] $\rho(r_c)$, $\nabla^2(r_c)$ and H are, respectively, the electron density, Laplacian of electron density and the total energy density at the BCP.

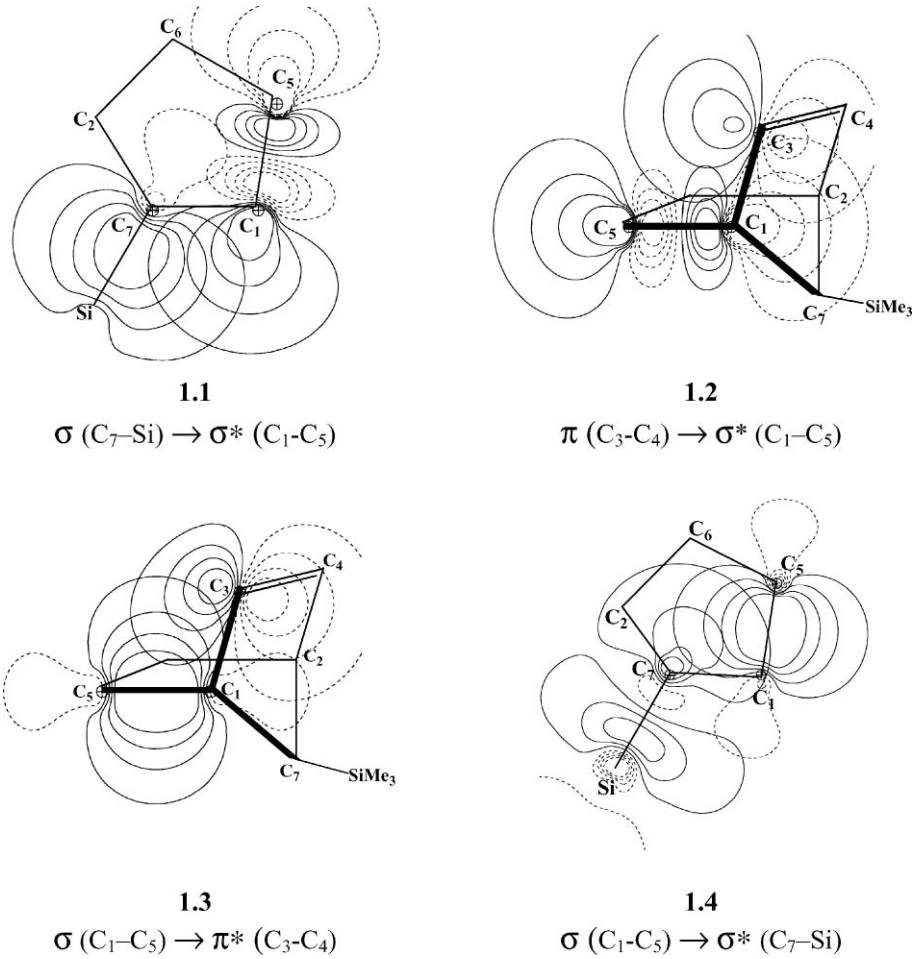

Fig. 1 Contour plots representing important two electron stabilizing orbital interactions generated with natural bond orbitals at the NBO/B3LYP/6-311+G**//6-31G* level.

C_2–C_6) bond, in concert with the findings based on NBO analyses. This prediction is further supported by Wiberg bond indices evaluated for the cycloadducts as well as the corresponding saturated bicyclic compounds (Table S3 in the ESI†). The calculated positive values for $\nabla^2\rho(r_c)$ indicate a locally depleted electron density between C_1 and C_5, characteristic of an ionic interaction. However, the total energy densities (H) are found to be uniformly negative, indicating a covalent interaction operating in the ground state. It has earlier been suggested that total energy density, H at the BCP is a better descriptor than $\nabla^2\rho(r_c)$ towards understanding the nature of bonding interactions.[30] Inspection of $\rho(r_c)$ values for the C_1–C_5 bonds for systems **1** to **19**, shows reasonable variations, depending on the nature of the antiperiplanar C_7-substituents. The degree of sensitivity of $\rho(r_c)$ values to the nature of the C_7-substituents could mean that the extent of ground state geometric distortion, particularly in the form of C_1–C_5 (and C_2–C_6) bond elongation, would contribute towards the energetic cost for carrying out rDA reactions. This is indeed found to be the case as revealed by good linear correlation between the free energies of activation and $\rho(r_c)$ values computed for C_1–C_5 bonds (Fig. 2).[31] For substrates that undergo a more facile rDA reaction, the $\rho(r_c)$ values were found to be lower. In general, the lower the $\rho(r_c)$ values for the incipient bond (reaction coordinate in the present case) the lower the activation barrier.[32]

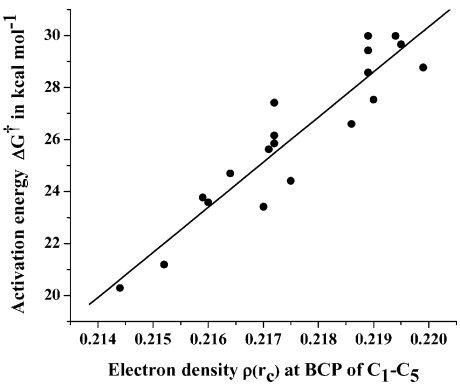

Fig. 2 Correlation between Gibbs free energies of activation (kcal mol^{-1}) and electron density $\rho(r_c)$ at bond critical points for **1** to **19** at the B3LYP/6-311+G**//B3LYP/6-31G* level.

After having carefully analyzed the electronic structure details of the ground state cycloadduct, we turned our attention to the dependence of activation energy for the rDA reaction on the nature of the C_7 substituent. The computed values for activation energy for a diverse set of substituted cycloadducts are included in Table 3. The lowest value for Gibbs free energy of activation for the cylcoreversion reaction is predicted to be for the –$SiMe_3$ substituted system (**1**), which amounts to 22.5 kcal mol^{-1}. Interestingly, the computed values obtained for adducts **1** and **7** are found to be in reasonable agreement with the available experimental reports. Experimental values of activation barrier for rDA reaction of **1** and **7** are, respectively, 24.8 ± 1 kcal mol^{-1} and 29 ± 1.5 kcal mol^{-1}.[13] Substituents such as –Si(Me)$_3$, –CHO, –PH_2, –BH_2 and –GeH_3, are also predicted to be effective in lowering the activation barrier compared to that with the unsubstituted system (X = H). Substituents such as nitro (**17**), hydroxyl (**18**) and fluoro (**19**) increases the activation barrier quite effectively. It is interesting to note that the ability of the σ(C_7–X) bond to serve as a donor orbital is critical to the rate enhancement rather than the nature of the substituents. For instance, substituents such as –NH_2 and –OMe can, in principle, act as electron donating groups, but are found to be not very effective in promoting the rDA reaction in the present case. A large number of such substituents are found to raise the activation barrier higher than 30 kcal mol^{-1}. Higher predicted activation energies imply that either prolonged heating or elevated temperature might be required to realize rDA reaction in such systems. Such generalizations could undoubtedly be valuable while resorting to experiments involving cycloreversion reactions.

Table 3 Energetics of retro Diels–Alder reaction of C_7 substituted cycloadducts at the B3LYP/6-311+G**//B3LYP/6-31G* level of theory

Substituents	$\Delta E^{\dagger}$	$\Delta H^{\dagger}_{298}$	$\Delta G^{\dagger}_{298}$	ΔH_{298}	ΔG_{298}
–$SiMe_3$ (**1**)	22.53	20.59	20.28	−0.11	−15.36
–GeH_3 (**2**)	23.37	21.35	21.19	0.47	−13.60
–BH_2 (**3**)	24.83	23.25	23.41	3.66	−10.62
–PH_2 (**4**)	25.84	23.82	23.58	3.90	−10.34
–CMe_3 (**5**)	26.74	24.59	23.77	3.58	−11.40
–CHO (**6**)	26.90	24.78	24.40	4.97	−9.55
–H (**7**)	27.50	25.28	24.69	6.84	−7.77
–C_2H_5 (**8**)	28.26	26.20	25.62	9.19	−4.79
–Me (**9**)	28.52	26.47	25.84	7.10	−7.64
–SH (**10**)	29.00	26.92	26.15	8.13	−6.77
–COMe (**11**)	29.63	27.51	26.59	5.75	−9.03
–COOH (**12**)	30.44	28.30	27.53	7.74	−7.14
–Cl (**13**)	30.28	28.17	27.41	8.91	−5.89
–NH_2 (**14**)	31.36	29.25	28.57	12.51	−2.39
–CN (**15**)	31.55	29.41	28.76	8.18	−6.55
–OMe (**16**)	32.37	30.08	29.42	11.45	−3.24
–NO_2 (**17**)	32.60	30.36	29.65	9.56	−5.41
–OH (**18**)	32.85	30.70	29.98	13.88	−1.08
–F (**19**)	32.80	30.67	29.98	12.10	−2.62

As pointed out in the earlier sections, the occupancy of σ*(C_1–C_5) [and C_2–C_6] is sensitive to the nature of the C_7-substituent.[33] We have noticed a fairly good correlation between the occupancy of the σ* orbital of the incipient bond and the free energy of activation of rDA reaction as depicted in Fig. 3(i). It is evidently clear from the plot that higher the occupancy of σ*(C_1–C_5), the lower the activation barrier. Thus, by examining the population of the antibonding orbital and degree of geometric distortion, such as bond elongation at the ground state, approximate estimates of the activation barrier can be obtained, without resorting to a full-fledged transition state search. The trends established in the present context can, perhaps, serve as a valuable generalization that could have wider implications on variety of rDA reactions. Further, the geometry of ground state cycloadduct will reflect the extent of delocalization and accompanying bond length variations, particularly the C_1–C_5 bond. Excellent correlation obtained between free energy of activation and C_1–C_5 bond length [Fig. 3(ii)] unequivocally establishes the importance of substituent-dependant ground state geometry changes on the reaction energetics of cycloreversion reactions.

Inspection of computed heats of the rDA reaction, (ΔH_{298}) at the B3LYP/6-311+G**//B3LYP/6-31G* level of theory conveys that the reaction is only slightly endothermic. Another factor relates to the entropic advantage accompanying the rDA reaction resulting in an overall exergonic transformation. Computed free

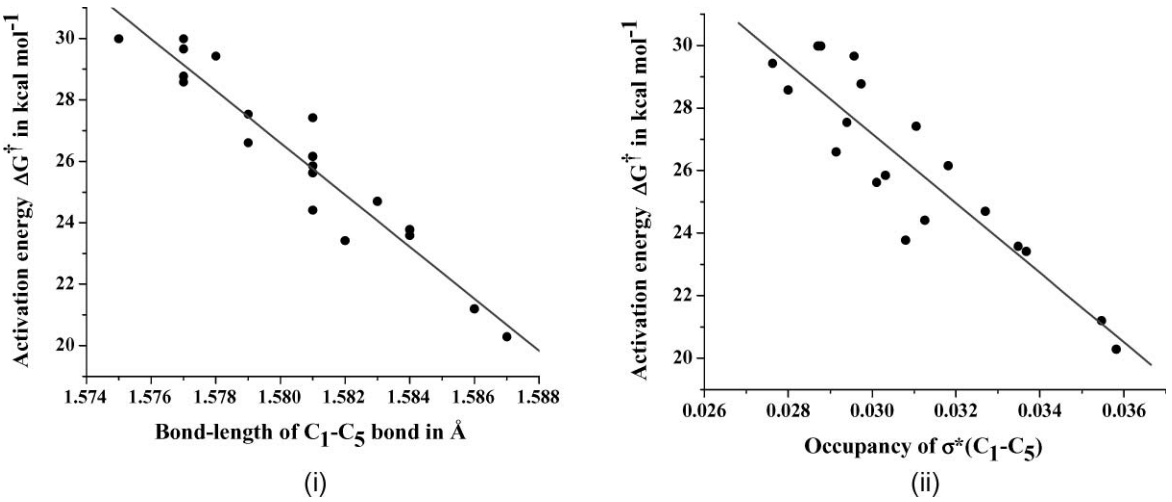

Fig. 3 Correlation between computed activation barrier (kcal mol^{-1}) and (i) bond length (**3·1**) (ii) occupancies of the C_1–C_5 bond (**3·2**).

energy changes for systems bearing C_7 substituents indicate that substituents that reduce the barrier to the rDA reaction (**1** to **6**, Table 3) compared to the unsubstituted system (**7**, when X = H) tend to be more exergonic while those that increase the barrier (**9** to **19**) are found to be less exergonic in nature. Starting from the transition state geometry, we have used a 10% displaced structure along the reaction coordinate (based on the imaginary vibrational frequency) so as to walk down from the transition state geometry by reoptimizing with stringent 'calcfc' option. It has also been noticed that the reactants (substituted cyclopentadiene and *p*-benzoquinone) tend to form a weakly interacting 'pre-reacting complex' near the exit channel. The heats of reactions are computed based on this stationary point on respective potential energy surfaces.

It can be anticipated that an elongated C_1–C_5 bond at the ground state will facilitate easier access to the transition state for the rDA reaction due to increased geometric similarity. In other words, if the ground state geometric distortion is along the reaction coordinate, the activation barrier is expected to be lower. White *et al.* have reported a similar analysis, in which they noticed a good correlation between the degree of bond lengthening and propensity towards cycloreversion reaction on a number of [2.2.2]-bicyclo systems.[34,14] Structural features at the transition states show additional significance in the context of the present discussion. Complete lists of geometrical parameters for the transition state structures are provided in Table 4. We intend to convey the importance of ground state structural distortions by taking representative examples. Optimized geometries of the transition state for the rDA reaction for selected cylcoadducts **1**, **7** and **19** are provided in Fig. 4. The C_1–C_5 distance in cycloadduct (**1**) and the transition state (**1**†) is 1.587 and 2.151 Å, respectively, a difference of only about 0.564 Å. Examination of geometry of the transition state for fluoro system (**19**†) reveals that C_1–C_5 bond distance is as high as 2.252, compared to 1.577 Å for **19**, indicating a loosely bound transition state bearing little structural similarity with the parent cycloadduct. Comparison of C_1–C_5 distances in the ground state and the corresponding transition state for the entire series (Table 1 and 4) of substituted cylcoadducts is useful in proposing interesting generalizations. It can be noticed

Table 4 Key structural parameters obtained at the B3LYP/6-31G* level for the transition state for rDA reaction of cycloadduct formed between substituted cyclopentadiene and *p*-benzoquinone[a]

Substituents	C_1–C_5	C_7–X	C_1–C_4	C_3–C_4	C_5–C_6
–$SiMe_3$(**1**)	2.151	1.944	1.419	1.387	1.420
–GeH_3 (**2**)	2.162	1.984	1.418	1.389	1.408
–BH_2 (**3**)	2.170	1.584	1.419	1.386	1.418
–PH_2 (**4**)	2.177	1.917	1.410	1.393	1.414
–CMe_3 (**5**)	2.192	1.582	1.405	1.398	1.413
–CHO (**6**)	2.185	1.542	1.411	1.396	1.412
–H (**7**)	2.200	1.103	1.405	1.399	1.410
–C_2H_5 (**8**)	2.198	1.555	1.405	1.400	1.410
–Me (**9**)	2.202	1.549	1.404	1.401	1.410
–SH (**10**)	2.212	1.865	1.403	1.403	1.411
–COMe (**11**)	2.183	1.559	1.406	1.399	1.411
–COOH (**12**)	2.218	1.525	1.403	1.401	1.410
–Cl (**13**)	2.230	1.845	1.398	1.406	1.409
–NH_2 (**14**)	2.227	1.474	1.397	1.409	1.406
–CN (**15**)	2.222	1.474	1.397	1.409	1.406
–OMe (**16**)	2.239	1.546	1.399	1.406	1.408
–NO_2 (**17**)	2.249	1.525	1.393	1.411	1.404
–OH (**18**)	2.245	1.426	1.394	1.415	1.404
–F (**19**)	2.252	1.400	1.391	1.415	1.403

[a] Atoms numbers are same as in Scheme 1.

that smaller the differences in C_1–C_5 bond distances between cycloadducts and transition states, the lower the activation barrier. This observation is in perfect concurrence with the Hammond postulate and underscores the importance of ground state bond elongation in rDA reactions.

We have tried to establish that substituents which tend to promote the rDA reaction (by lowering the activation barrier) offer significant modulation of the ground state structural features of the molecule. Ground state bond elongation in the present systems gets translated in the form of a lower activation barrier and tighter binding between the departing fragments. In order to gain additional insights on how tightly held are the diene and the dienophile at the transition state, we have decided to examine the topological features with the help of electron density at (3, −1) bond critical points using the AIM method. As anticipated, the

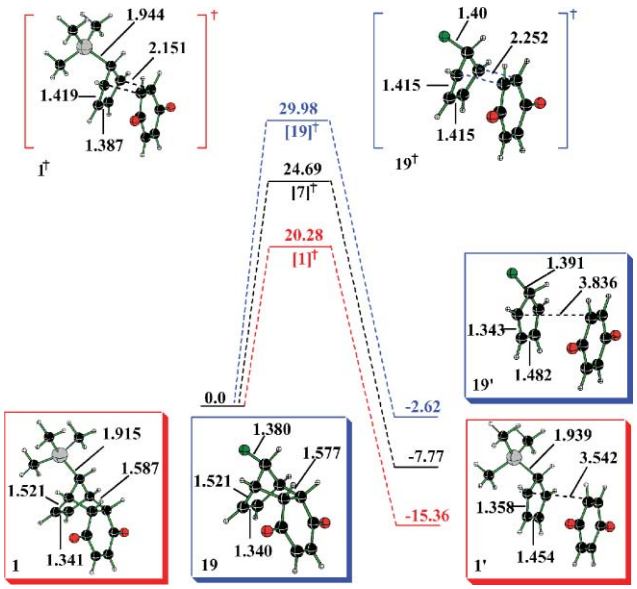

Fig. 4 Gibbs free energy profile of the rDA reaction for **1** (X = – $SiMe_3$), **7** (X = H) and **19** (X = F) computed at the B3LYP/6-311+G**//B3LYP/6-31G* level.

computed $\rho(r_c)$ values for the C_1–C_5 bond for the transition states are found to be generally much lower than the corresponding cycloadducts. The highest and lowest $\rho(r_c)$ values are predicted for **1**† and **19**†, respectively. Moreover, the $\rho(r_c)$ values are found to decrease quite steadily from **1** to **19**, indicating rather weakly-bound transition states for the rDA reaction where the activation barrier is higher [computed $\rho(r_c)$ values are provided in the ESI†, Table S4]. Uniformly negative values for the total energy densities (H) between C_1–C_5 at the transition state, across range of substituted cycloadducts (**1**† through **19**†), indicate the covalent nature of the transition states in these reactions.

Conclusion

The density functional theory studies on the reaction profile for an important class of retro Diels–Alder reactions involving cycloadducts formed between substituted cyclopentadiene and *p*-benzoquinone revealed the importance of ground state bond elongation on the reaction profile. The nature of the substituents present on the methano bridge is found to be crucial to bond elongation as revealed by $\sigma(C_7–X)$ to $\sigma^*(C_1–C_5)$ [and $\sigma^*(C_2–C_6)$] orbital delocalizations. Substituents such as $–SiMe_3$ are found to be effective in lowering the activation barrier by significantly populating the C_1–C_5 antibonding orbital at the ground state cycloadduct. A fairly good correlation between (i) occupancy of $\sigma^*(C_1–C_5)$ [and $\sigma^*(C_2–C_6)$] and (ii) C_1–C_5 bond elongation with the activation barrier evidently establishes the importance of ground state geometric distortion (resulting from two-electron stabilizing interactions) on the cycloreversion reactions. Topological analyses of electron density at the C_1–C_5 bond critical point $\rho(r_c)$ exhibited a linear correlation with the free energies of activation. For substrates that undergo relatively facile rDA reaction, the $\rho(r_c)$ values are found to be lower.

Acknowledgements

We acknowledge the computer center, IIT Bombay for computing facilities. MP acknowledges CSIR-New Delhi for senior research fellowship. We thank Professors S. R. Kotha and K. D. Deodhar for valuable discussions during the course of this work.

References

1 O. Diels, K. Alder and E. Naujoks, *Ber. Dtsch. Chem. Ges. B*, 1929, **62**, 554–562.

2 (*a*) H. Kwart and K. King, *Chem. Rev.*, 1968, **68**, 415–447; (*b*) J. L. Ripoll, A. Rouessac and F. Rouessac, *Tetrahedron*, 1978, **34**, 19–40; (*c*) M. C. Lasne and J. L. Ripoll, *Synthesis*, 1985, 121–143; (*d*) A. Ichihara, *Synthesis*, 1987, 207–222; (*e*) T. H. Kurniadi, R. B. Rhlid, M.-A. Juillerat, T. Gefflaut, J. Bolte and R. G. Berger, *Tetrahedron*, 2003, **59**, 6109–6112; (*f*) K. Suzuki, K. Inomata and Y. Endo, *Org. Lett.*, 2004, **6**, 409–411; (*g*) G. Stájer, F. Miklós, I. Kanizsai, F. Csende, R. Sillanpää and P. Sohár, *Eur. J. Org. Chem.*, 2004, 3701–3706; (*h*) D. Branowska, *Tetrahedron*, 2004, **60**, 6021–6027; (*i*) Y. Inokuma, T. Matsunari, N. Ono, H. Uno and A. Osuka, *Angew. Chem., Int. Ed.*, 2005, **44**, 1856–1860.

3 (*a*) A. J. H. Klunder, J. Zhu and B. Zwanenburg, *Chem. Rev.*, 1999, **99**, 1163–1190; (*b*) J. C. C. Atherton and S. Jones, *Tetrahedron Lett.*, 2002, **43**, 9097–9100; (*c*) K. L. Burgess, N. J. Lajkiewicz, A. Sanyal, W. Yan and J. K. Snyder, *Org. Lett.*, 2005, **7**, 31–34; (*d*) N. R. Conley, R. J. Hung and C. G. Willson, *J. Org. Chem.*, 2005, **70**, 4553–4555.

4 D. N. Reinhoudt and C. G. Kouwenhoven, *Tetrahedron Lett.*, 1974, **25**, 2163–2166.

5 P. J. Boul, P. Reutenauer and J. Lehn, *Org. Lett.*, 2005, **7**, 15–18.

6 J. R. McElhanon and D. R. Wheeler, *Org. Lett.*, 2001, **3**, 2681–2683.

7 (*a*) J. Sauer and R. Sustmann, *Angew. Chem., Int. Ed. Engl.*, 1980, **19**, 773–801; (*b*) K. N. Houk, Y. Li and J. D. Evanseck, *Angew. Chem., Int. Ed. Engl.*, 1992, **31**, 682–708; (*c*) S. M. Bachrach, *J. Org. Chem.*, 1995, **60**, 4395–4398; (*d*) K. N. Houk, J. Gonzalez and Y. Li, *Acc. Chem. Res.*, 1995, **28**, 81–90; (*e*) O. Wiest, D. C. Montiel and K. N. Houk, *J. Phys. Chem. A*, 1997, **101**, 8378–8388; (*f*) J. T. Manka, A. G. Douglass, P. Kaszynski and A. C. Friedli, *J. Org. Chem.*, 2000, **65**, 5202–5206; (*g*) M. L. McKee, *J. Am. Chem. Soc.*, 2001, **123**, 9426–9435; (*h*) E. Kraka, A. Wu and D. Cremer, *J. Phys. Chem. A*, 2003, **107**, 9008–9021; (*i*) A. G. Leach, K. N. Houk and J. Reymond, *J. Org. Chem.*, 2004, **69**, 3683–3692; (*j*) Z.-X. Yu, Q. Dang and Y.-D. Wu, *J. Org. Chem.*, 2005, **70**, 998–1005.

8 (*a*) K. N. Houk, *J. Am. Chem. Soc.*, 1973, **95**, 4092–4094; (*b*) K. N. Houk, *Acc. Chem. Res.*, 1975, **8**, 361–369; (*c*) O. Eisenstein, J. M. Lefour, N. T. Anh and R. F. Hudson, *Tetrahedron*, 1977, **33**, 523–531; (*d*) S. D. Kahn, F. Pau, L. E. Overman and W. J. Hehre, *J. Am. Chem. Soc.*, 1986, **108**, 7381–7396; (*e*) L. Rulisek, P. Sebek, Z. Havlas, R. Hrabal, P. Capek and A. Svatos, *J. Org. Chem.*, 2005, **70**, 6295–6302.

9 (*a*) J. B. Macaulay and A. G. Fallis, *J. Am. Chem. Soc.*, 1987, **109**, 663–666; (*b*) J. M. Coxon and D. Q. McDonald, *Tetrahedron Lett.*, 1992, **33**, 651–654; (*c*) R. A. Poirier, C. C. Pye, J. D. Xidos and D. J. Burnell, *J. Org. Chem.*, 1995, **60**, 2328–2329.

10 (*a*) J. W. Storer, L. Raimondi and K. N. Houk, *J. Am. Chem. Soc.*, 1994, **116**, 9675–9683; (*b*) B. R. Beno, K. N. Houk and D. A. Singleton, *J. Am. Chem. Soc.*, 1996, **118**, 9984–9985; (*c*) K. N. Houk, B. R. Beno, M. Nendel, K. Black, H. Y. Yoo, S. Wilsey and J. K. Lee, *J. Mol. Struct. (THEOCHEM)*, 1997, **398–399**, 167–179; (*d*) J. Tian, K. N. Houk and F. G. Klarner, *J. Phys. Chem. A*, 1998, **102**, 7662–7667; (*e*) D. A. Singleton, B. E. Schulmeier, C. Hang, A. A. Thomas, S. Leung and S. R. Merrigan, *Tetrahedron*, 2001, **57**, 5149–5160; (*f*) C. Delamere, C. Jakins and E. Lewars, *J. Mol. Struct. (THEOCHEM)*, 2002, **593**, 79–91.

11 K. N. Houk, Y.-L. Lin and F. K. Brown, *J. Am. Chem. Soc.*, 1986, **108**, 554–556.

12 (*a*) B. A. Horn, J. L. Herek and A. H. Zewail, *J. Am. Chem. Soc.*, 1996, **118**, 8755–8756; (*b*) E. W.-G. Diau, S. D. Feyter and A. H. Zewail, *Chem. Phys. Lett.*, 1999, **304**, 134–144; (*c*) K. E. Wise and R. A. Wheeler, *J. Phys. Chem. A*, 1999, **103**, 8279–8287.

13 P. Magnus, P. M. Cairns and J. Moursounidism, *J. Am. Chem. Soc.*, 1987, **109**, 2469–2471.

14 D. Birney, T. K. Lim, J. H. P. Koh, B. R. Pool and J. M. White, *J. Am. Chem. Soc.*, 2002, **124**, 5091–5099.

15 S. Kotha, S. Banerjee, M. P. Patil and R. B. Sunoj, *Org. Biomol. Chem.*, 2006, **4**, 1854–1856.
16 (*a*) M. J. Frisch, G. W. Trucks, H. B. Schlegel, G. E. Scuseria, M. A. Robb, J. R. Cheeseman, V. G. Zakrzewski, J. A. Montgomery, Jr., R. E. Stratmann, J. C. Burant, S. Dapprich, J. M. Millam, A. D. Daniels, K. N. Kudin, M. C. Strain, O. Farkas, J. Tomasi, V. Barone, M. Cossi, R. Cammi, B. Mennucci, C. Pomelli, C. Adamo, S. Clifford, J. Ochterski, G. A. Petersson, P. Y. Ayala, Q. Cui, K. Morokuma, P. Salvador, J. J. Dannenberg, D. K. Malick, A. D. Rabuck, K. Raghavachari, J. B. Foresman, J. Cioslowski, J. V. Ortiz, A. G. Baboul, B. B. Stefanov, G. Liu, A. Liashenko, P. Piskorz, I. Komaromi, R. Gomperts, R. L. Martin, D. J. Fox, T. Keith, M. A. Al-Laham, C. Y. Peng, A. Nanayakkara, M. Challacombe, P. M. W. Gill, B. G. Johnson, W. Chen, M. W. Wong, J. L. Andres, C. Gonzalez, M. Head-Gordon, E. S. Replogle and J. A. Pople, *GAUSSIAN 98 (Revision A.11)*, Gaussian, Inc., Pittsburgh, PA, 2001; (*b*) A. D. Becke, *J. Chem. Phys.*, 1993, **98**, 5648–5652; (*c*) A. D. Becke, *Phys. Rev. A*, 1988, **38**, 3098–3100; (*d*) C. Lee, W. Yang and R. G. Parr, *Phys. Rev. B*, 1988, **37**, 785–789.
17 (*a*) D. A. Hrovat, J. Chen, K. N. Houk and W. T. Borden, *J. Am. Chem. Soc.*, 2000, **122**, 7456–7460; (*b*) V. Guner, K. S. Khoung, A. G. Leach, P. S. Lee, M. D. Bartberger and K. N. Houk, *J. Phys. Chem.*, 2003, **107**, 11445–11459; (*c*) V. A. Guner, K. N. Houk and I. W. Davies, *J. Org. Chem.*, 2004, **69**, 8024–8028; (*d*) H. Shuichi, D. A. Hrovat and W. T. Borden, *J. Am. Chem. Soc.*, 2004, **126**, 10028–10034; (*e*) K. S. Khuong, C. M. Beaudry, D. Trauner and K. N. Houk, *J. Am. Chem. Soc.*, 2005, **127**, 3688–3689.
18 A. P. Scott and L. Radom, *J. Phys. Chem.*, 1996, **100**, 16502–16513.
19 (*a*) C. Gonzalez and H. B. Schlegel, *J. Chem. Phys.*, 1989, **90**, 2154–2161; (*b*) C. Gonzalez and H. B. Schlegel, *J. Phys. Chem.*, 1990, **94**, 5523–5527.
20 (*a*) F. Weinhold, in *Encyclopedia of Computational Chemistry, vol. 3*, ed. P. v. R. Schleyer, New York, 1998, p. 1792; (*b*) A. E. Reed, L. A. Curtiss and F. Weinhold, *Chem. Rev.*, 1988, **88**, 899–926.
21 R. F. W. Bader, *Atoms in Molecules: A Quantum Theory*, Clarendon Press, Oxford, 1990.
22 (*a*) F. Biegler-Konig, J. Schonbohm and D. Bayles, *J. Comput. Chem.*, 2001, **22**, 545; (*b*) F. Biegler-Konig and J. Schonbohm, *J. Comput. Chem.*, 2002, **23**, 1489.
23 (*a*) J. B. Lambert, *Tetrahedron*, 1990, **46**, 2677–2689; (*b*) J. B. Lambert, Y. Zhao, R. W. Emblidge, L. A. Salvador, X. Liu, J. So and E. C. Chelius, *Acc. Chem. Res.*, 1999, **32**, 183–190.
24 In case of those substituents that could exist as different rotamers (around the C_7–X bond, X for first atom of the substituent) the conformer with lowest energy is taken into consideration for the present discussion. Information on other conformers is provided in the ESI† (Table S8).
25 Please see the ESI† (Table S1) for a complete list of structural parameters for both the cycloadducts and saturated bicyclic compounds considered in this study.
26 (*a*) S. J. Wilkens, W. M. Westler, F. Weinhold and J. L. Markley, *J. Am. Chem. Soc.*, 2002, **124**, 1190–1191; (*b*) S. Eduardo and B. Gerado, *J. Phys. Chem. A*, 2003, **107**, 5544–5554; (*c*) I. V. Alabugin and M. Manoharan, *J. Org. Chem.*, 2004, **69**, 9011–9024; (*d*) M. Takahashi and K. Sakamoto, *J. Phys. Chem. A*, 2004, **108**, 5710–5714.
27 (*a*) S. Tomoda, *Chem. Rev.*, 1999, **99**, 1243–1264; (*b*) S. Tomoda and S. Takatoshi, *Chem. Commun.*, 1999, 423–424.
28 Delocalizations were analyzed based on second order perturbation energy values obtained with the NBO/B3LYP/6-311+G**//B3LYP/6-31G* level. Please see the ESI† (Table S2) for details on all four kinds of delocalizations discussed here.
29 Based on AIM/B3LYP/6-311+G**//B3LYP/6-31G* calculations on the saturated bicyclic compounds. Please see the ESI† (Table S3) for further details on the saturated compounds.
30 (*a*) W. Koch, G. Frenking, J. Gauss, D. Cremer and J. R. Collins, *J. Am. Chem. Soc.*, 1987, **109**, 5917–5934; (*b*) I. Rozas, I. Alkorta and J. Elguero, *J. Am. Chem. Soc.*, 2000, **122**, 11154–11161.
31 Based on the Gibbs free energy of activation and the free energy of reaction, we have carried out a Marcus-type analysis by first calculating the intrinsic free energy of activation. Correlations between intrinsic free energies and structural parameters are found to be nearly identical to those obtained using the Gibbs free energy of activation. These results are summarized in the ESI† (Table S5, Figures S1 and S2).
32 Based on the AIM/B3LYP/6-311+G**//B3LYP/6-31G* calculations on the cycloadducts. Please see the ESI† (Table S3).
33 The occupancies of bonding the $\sigma(C_1–C_5)$ orbital remained nearly the same, irrespective of the nature of substituent present at C_7. Please see the ESI† (Table S2).
34 B. R. Pool and J. M. White, *Org. Lett.*, 2000, **2**, 3505–3507.

